The L_2 Polynomial Spline Pyramid

Michael Unser, *Member, IEEE*, Akram Aldroubi, and Murray Eden, *Life Fellow, IEEE*

***Abstract*—The first part of this paper is concerned with the derivation of general methods for the L_2 approximation of signals by polynomial splines. Such approximations can be represented in a variety of ways using different sets of shift-invariant basis functions (e.g., cardinal, dual, orthogonal or standard B-splines). The main result is that the expansion coefficients of the approximation are obtained by linear filtering and sampling.**

The second part applies those results to construct a L_2 polynomial spline pyramid that is a parametric multiresolution representation of a signal. This hierarchical data structure is generated by repeated application of a REDUCE function (prefilter and downsampler). A complementary EXPAND function (up-sampler and post-filter) allows a finer resolution mapping of any coarser level of the pyramid. Four equivalent representations of this pyramid are considered, and the corresponding REDUCE and EXPAND filters are determined explicitly for polynomial splines of any order n (odd). Some image processing examples are presented. The present formulation provides a number of interesting links with several other multiresolution techniques including the wavelet transform, scale-space filtering, and Burt's Gaussian and Laplacian pyramids. In particular, we demonstrate that the performance of the Laplacian pyramid can be improved significantly by using a modified EXPAND function associated with the dual representation of a cubic spline pyramid.

***Index Terms*—Binomial filters, B-splines, decimation, interpolation, multigrid methods, multiresolution, polynomial splines, pyramid, recursive filters, scale space, signal approximation, spline filters, wavelet transform.**

I. Introduction

IMAGE PYRAMIDS are data structures for representing image copies at multiple resolutions [1]. These representations are particularly useful for improving the efficiency of many image processing tasks such as edge detection [2], object recognition, and image segmentation [1], [3]. Their main advantage is to provide a simple mechanism for adjusting the spatial resolution to optimize the performance of image processing algorithms that operate on very localized neighborhoods with a fixed number of pixels. Furthermore, the use of a coarse-to-fine strategy can dramatically improve the execution speed and convergence properties of iterative algorithms that proceed by successive refinement. Over the past ten years, these concepts have caught the attention of the mathematical community and have led to the development of powerful multigrid methods for solving a variety of elliptic boundary value problems [4]. Some specialized forms of these multigrid relaxation techniques have been used to find numerical solutions for differential equations that arise in the context of computer vision, for example, visible surface interpolation [5], [6] or optical flow determination [7], [8].

Image pyramids are also frequently used for generating multiscale descriptions of signals or images. Instead of keeping a full copy of each resolution level, some researchers have found it useful to code the differences between resolution levels. Examples of such bandpass representations are Burt's Laplacian pyramid [9], Crowley's difference of low-pass transform [10], the class of pyramid structures used in subband coding [11], [12], and the recently proposed wavelet transform [13], [14]. Many of these approaches have proven to be particularly effective for image coding [9], [12]. Other examples of applications include feature extraction [15] and texture analysis [13], [16].

A related method of multiresolution analysis is the decomposition of a signal in scale space by repeated convolution with Gaussian kernels of increasing width [17]-[19]. The main characteristic usually analyzed is the systematic behavior of the extrema (or zero crossings of the Laplacian) as a function of scale [20]. Koenderink has pointed out several striking correspondences between important scale-space characteristics and properties of the visual system, such as size invariance and the presence of multiple frequency-tuned channels [18]. An axiomatic formulation of a scale-space theory for discrete signals, in which continuous Gaussian filters are replaced by generalized binomial kernels, has been proposed recently [21].

The construction of an image pyramid involves the repeated application of a REDUCE function that reduces the image by a factor of two. The reverse of this operation is obtained through the EXPAND function, which maps (or extrapolates) a coarser level onto a finer sampling grid. The REDUCE and EXPAND functions (or DOWN and UP in the multigrid literature) can be implemented using a combination of digital filters and sampling rate converters; the convolution operators used in both cases are usually identical. An important requirement in the design of such systems is that the loss of information occurring during resolution conversion be minimal. Clearly, the REDUCE operation should be chosen such that lower resolution copies remain as close as possible to the original image in order to ensure the compatibility between image processing operations performed at different resolutions. Moreover, the EXPAND function should be designed to minimize the approximation error between the original image and an extrapolation obtained from a coarser level of the pyramid. As surprising as this may appear, some of the most frequently used combinations of REDUCE and EXPAND functions (see, for example, [4] and [9]) are not consistent with this last requirement. A notable exception is the orthogonal multiresolution representation associated with the wavelet decomposition described by Mallat [14].

Manuscript received December 4, 1990; revised October 28, 1991. Recommended for acceptance by Associate Editor S. Tanimoto.

The authors are with the Biomedical Engineering and Instrumentation Program, National Center for Research Resources, National Institutes of Health, Bethesda, MD 20892.

IEEE Log Number 9206551.

The objective of this paper is to develop a coherent approach to the multiresolution representation of signals such as to minimize loss of information between resolution levels. An important requirement is to use the smallest number of samples possible at each scale in order to 1) provide a compact multiscale representation and 2) improve the efficiency of processing algorithms. For this purpose, we will consider the generation of a class of polynomial spline pyramids that fall within the general framework of the multiresolution transform defined by Mallat. An important aspect of this study will be to investigate polynomial spline representations that are not necessarily orthogonal such as the standard B-spline representation [22] or the cardinal representation in terms of sampled values [23]. This point of view will result in the definition of modified REDUCE and EXPAND functions using complementary–but not necessarily identical–filters. This formulation will bring out filter structures that are similar, if not identical, to the operators used by Burt, Witkin, and others, thus establishing a close relationship with some of the approaches mentioned above.

Polynomial splines of order n are piecewise polynomials that are connected to guarantee the continuity of the function and its derivatives up to order $n-1$. These functions, which were introduced and studied extensively by Schoenberg [22], [24], can be expressed as weighted sums of shifted B-spline basis functions. In the case of equally spaced data points, the B-spline interpolation problem can be solved efficiently using recursive filters [25]. Moreover, an increase in the order of the splines provides a progressive shift from the simple zero order and piecewise linear methods of interpolation to the ideal "sinc" interpolation for bandlimited signals; these extreme cases correspond to polynomial spline interpolations of order $n = 0, n = 1$, and $n \to +\infty$, respectively [23], [26], [27]. Additional features that should make splines attractive for computer vision are as follows:

1. Polynomial splines have good regularity properties. Among all interpolants of a given degree of smoothness, they are those that oscillate the least [28]. Precise convergence rates for the approximation of smooth functions and their derivatives by splines are also available [29].
2. Polynomial splines have a simple explicit form that makes them easy to manipulate. Operations such as derivation and integration can be performed in a straightforward manner. Polynomial splines therefore constitute the method of choice for designing finite element methods for the numerical solution of differential equations [28].

These properties should simplify the development of algorithms for computer vision problems that are better formulated in a continuous framework (e.g., edge detection, feature extraction) or can be specified in terms of differential equations (optical flow, surface reconstruction, shape for shading, etc.) [30].

The presentation is organized as follows. Section II introduces some preliminary concepts and definitions; it also provides a review of the main properties of discrete B-spline filters. The general problem of the minimum error approximation of an arbitrary function in L_2 using polynomial splines with a step size m is solved in Section III. These mathematical results are then used in Section IV to construct the polynomial spline pyramid, which provides a series of multiresolution signal approximations with an octave scale progression. Some experimental image processing examples and comparisons with other methods are presented in Section V. The final part is a discussion of the main results of this paper and how they relate to previous approaches.

II. PRELIMINARIES

In this section, we first consider a series of transformations that operate on discrete l_2 sequences (or signals) and describe their effect in the z-transform domain. We then define the function spaces that will be considered in this paper and recall some important properties of discrete B-spline kernels, which play an essential role in the derivation of spline filters.

A. Discrete l_2 Sequences

l_2 is the vector space of square-summable sequences $a(k), k \in \mathbf{Z}$. Any sequence $a \in l_2$ is uniquely characterized by its z-transform, which we denote by a capital letter:

$$A(z) = \sum_{k=-\infty}^{+\infty} a(k) z^{-k}.$$

This correspondence is also expressed as $a(k) \overset{z}{\longleftrightarrow} A(z)$. The Fourier transform is obtained by simply replacing z by $e^{j2\pi f}$. The convolution between two discrete sequences $a \in l_2$ and $b \in l_2$ is

$$b * a(k) = \sum_{l=-\infty}^{+\infty} b(l) a(k-l) \overset{z}{\longleftrightarrow} B(z)A(z).$$

It is sometimes useful to view b as the impulse response of a shift-invariant filtering operator that is applied to $a(k)$. This operator is entirely described by its transfer function $B(z)$. If $B(z) \neq 0$ is a polynomial with complex roots that are not on the unit circle, the inverse operator $(b)^{-1}$ exists and is uniquely defined by the equation

$$\forall k \in \mathbf{Z}, \qquad (b)^{-1} * b(k) = \delta_0(k)$$

where $\delta_0(k)$ denotes the unit pulse at the origin. We also define the square-root inverse operator $(b)^{-1/2}$ (if it exists):

$$(b)^{-1/2}(k) \overset{z}{\longleftrightarrow} B(z)^{-1/2}.$$

Another operator is the up-sampling by an integer multiple m, which is defined as

$$\forall k \in \mathbf{Z}, \qquad [b]_{\uparrow m}(k) := \begin{cases} b(k') & \text{for } k = mk' \\ 0 & \text{otherwise} \end{cases} \overset{z}{\longleftrightarrow} B(z^m).$$

The dual operation is the decimation by an integer factor m:

$$\forall k \in \mathbf{Z}, \quad [b]_{\downarrow m}(k) := b(mk) \overset{z}{\longleftrightarrow} \frac{1}{m} \sum_{k=0}^{m-1} B\left(\left[z e^{j2\pi k}\right]^{1/m}\right).$$

B. Function Spaces

L_2 denotes the space of measurable, square-integrable, functions $g(x)$, $x \in \mathbb{R}$. The inner product of two functions $g \in L_2$ and $h \in L_2$ is

$$\langle g(x), h(x) \rangle = \int_{-\infty}^{+\infty} g(x)h(x)dx.$$

In this paper, we will be concerned with the problem of constructing polynomial spline approximations of $g(x)$. The generic space of polynomial splines of order n is denoted by $\mathbf{S}_1^n$, where the superscript n refers to the degree of the polynomial segments and where the subscript represents the spacing between the knot points (i.e., the joining points of the polynomial segments). More precisely, $\mathbf{S}_1^n$ is the subset of functions in L_2 that are of class $\mathbb{C}^{n-1}$ (i.e., continuous functions with continuous derivatives up to order $n-1$) and are equal to a polynomial of degree n on each interval $[k, k+1), k \in \mathbf{Z}$ when n is odd, and $[k-1/2, k+1/2), k \in \mathbf{Z}$ when n is even. $\mathbf{S}_1^n$ is a closed vector space and can be defined as (see Theorem 12, p. 199, of [22]):

$$\mathbf{S}_1^n = \left\{ g^n(x) = \sum_{k=-\infty}^{+\infty} c(k)\beta^n(x-k) | c \in l_2 \right\} \tag{2.1}$$

where $\beta^n(x)$ is the central B-spline of order n

$$\beta^n(x) := \sum_{j=0}^{n+1} \frac{(-1)^j}{n!} \binom{n+1}{j} \left[x + \frac{n+1}{2} - j \right]_+^n, \quad (x \in \mathbb{R}) \tag{2.2}$$

with the convention that $[x]_+ = \max\{0, x\}$. The Fourier transform of $\beta^n(x)$ is given by

$$B^n(f) = [\mathrm{sinc}(f)]^{n+1} \tag{2.3}$$

where $\mathrm{sinc}(x) := \sin(\pi x)/\pi x$.

To obtain a multiscale representation of $g(x) \in L_2$, we will consider polynomial spline functions with different spacings Δ between the knot points. The corresponding function spaces can be defined by simple scaling. In other words, if $g(x) \in \mathbf{S}_1^n$, then $g_\Delta(x) := g(x/\Delta)$, where Δ is strictly positive, is an element of $\mathbf{S}_\Delta^n$, which is defined as

$$\mathbf{S}_\Delta^n = \left\{ g_\Delta^n(x) = \sum_{k=-\infty}^{+\infty} c_\Delta(k)\beta_\Delta^n(x - k\Delta), | c_\Delta \in l_2 \right\} \tag{2.4}$$

where $\beta_\Delta^n(x) := \beta^n(x/\Delta)$. The spacing between the knot points Δ, which is also referred to as the sampling step or resolution, determines the quality of the approximation of a given function $g(x)$. As Δ tends to zero, the L_2-approximation error vanishes [29], which is also equivalent to say that the union of sets $\cup_{\Delta \in R^+} \mathbf{S}_\Delta^n$, is dense in L_2.

For simplicity, we will assume that the smallest spacing for a multiresolution representation is unity and restrict the analysis to integer values of Δ. Thus, we can define the multiresolution spline decomposition of a function $g(x) \in L_2$ associated with the increasing scale progression $S = \{m_1, \cdots, m_k, \cdots\}$ as the sequence of minimum error approximations of $g(x)$: $g_{m_1}^n(x) \in \mathbf{S}_{m_1}^n$, $g_{m_2}^n(x) \in \mathbf{S}_{m_2}^n, \cdots, g_{m_k}^n(x) \in \mathbf{S}_{m_k}^n, \cdots$. The polynomial spline pyramid is associated with the scale progression $S = \{1, 2, \cdots, 2^k, \cdots\}$, which corresponds to a doubling of the resolution at each step. When n and m are not both even, the corresponding subspaces are embedded in each other since it can be shown that $\mathbf{S}_{m\Delta}^n \subset \mathbf{S}_\Delta^n$ for any positive integer m such that the product $(n+1)(m-1)$ is even.

To illustrate the fact that polynomial spline subspaces are nested when the step size is increased by a power of two, we consider a function that is piecewise linear over each interval $[k \cdot 2^i, (k+1) \cdot 2^i], k \in \mathbf{Z} : g_{(i)}^1(x) \in \mathbf{S}_{2^i}^1$. Clearly, $g_{(i)}^1$ is also piecewise linear over the sequence of smaller intervals $[k \cdot 2^j, (k+1) \cdot 2^j], k \in \mathbf{Z}$, where $j < i$. Hence $g_{(i)}^1(x) \in \mathbf{S}_{2^j}^1$ for $j \leq i$, which also implies that $\cdots \supset \mathbf{S}_{2^0}^1 \supset \mathbf{S}_{2^1}^1 \cdots \supset \mathbf{S}_{2^i}^1$.

C. Discrete B-spline Filters

Discrete B-spline kernels are obtained by sampling the continuous B-spline functions $\beta^n(x)$. These sequences play a crucial role in the design of digital filters for B-spline interpolation and approximation [25], [31]. The impulse response of the so-called indirect B-spline filter of order n is

$$b^n(k) := \beta^n(k) \qquad \forall k \in \mathbf{Z} \tag{2.5}$$

The expanded (or interpolated) version of this kernel by an integer factor of m is

$$b_m^n(k) := \beta^n(k/m) \qquad \forall k \in \mathbf{Z}. \tag{2.6}$$

Except for the case when n and m are both even, we have shown previously that the expanded B-spline kernels satisfy the convolution property [25]

$$b_m^n(k) = u_m^n * b^n(k) \qquad \forall k \in \mathbf{Z} \tag{2.7}$$

where $u_m^n(k)$ is a symmetric sequence that corresponds to the impulse response of a cascade of $(n+1)$ moving average filters of length m. More precisely, the transfer function of u_m^n can be factorized as

$$U_m^n(z) = \frac{z^{k_0}}{m^n} \left(\sum_{k=0}^{m-1} z^{-k} \right)^{n+1} \tag{2.8}$$

where $k_0 = (n+1)(m-1)/2$ is a proper offset that makes the global response symmetrical. The direct B-spline filter of order n is defined in [25] as

$$(b^n)^{-1}(k) \overset{z}{\longleftrightarrow} B_1^n(z)^{-1} = \frac{1}{b^n(0) + \sum_{k=1}^{(n+1)/2} b^n(k)(z^k + z^{-k})} \tag{2.9}$$

and has been shown to be stable for any value of n [23]. An equivalent characterization of this operator in Fourier space is

$$B_1^n(e^{j2\pi f})^{-1} = \frac{1}{\sum_{k=-\infty}^{+\infty} [\mathrm{sinc}(f-k)]^{n+1}} \tag{2.10}$$

which can be directly derived from (2.5) and (2.3). Some examples of spline filters that will be useful are given in Table I.

TABLE I
FILTERS FOR THE BILINEAR AND CUBIC SPLINE PYRAMIDS

Impulse response	Transfer function	Type	Poles : $\{\|z_i\|<1, i=1,..,[n/2]\}$
$b^1(k)$	1	id.	-
$b^3(k)$	$\frac{1}{6}(z+4+z^{-1})$	FIR	-
$b^7(k)$	$\frac{1}{5040}(2416+1191[z+z^{-1}]+120[z^2+z^{-2}]+z^3+z^{-3})$	FIR	-
$u_2^1(k)$	$\frac{1}{2}(z+2+z^{-1})$	FIR	-
$u_2^3(k)$	$\frac{1}{8}(z^2+4z+6+4z^{-1}+z^{-2})$	FIR	-
$(b^3)^{-1}(k)$	$\frac{6}{z+4+z^{-1}}$	IIR	$z_1 = -2+\sqrt{3} = -0.267949$
$(b^7)^{-1}(k)$	$\frac{5040}{z^3+120z^2+1191z+2416+1191z^{-1}+120z^{-2}+z^{-3}}$	IIR	$z_1=-0.53528$ $z_2=-0.122555$ $z_3=-0.009144869$

D. Generalizations to Higher Dimensions

Although the theoretical presentation is concerned with 1-D signals only, all subsequent results are directly applicable in higher dimensions through the use of tensor product splines [29]. The corresponding basis functions are obtained from the product of 1-D splines defined for each index variable. Since all basis functions are separable, the corresponding transformations are also separable [32]. This implies that higher dimensional versions of all algorithms that will be described can be implemented by successive 1-D processing along the coordinates.

III. B-Spline Representations and Approximations

Our motivation for representing a function $g(x) \in L_2$ in terms of polynomial splines is to achieve data reduction. This process is a particular form of discretization since $g^n(x)$ is entirely characterized by the l_2 sequence of its B-spline coefficients. We also note that there is a reduction in the number of samples by a factor of m between a coarse representation in $\mathbf{S}_m^n$ and a finer one in $\mathbf{S}_1^n$.

In this section, we introduce a series of equivalent representations of splines using different sets of shift-invariant basis functions. We then derive general computational procedures for the multiresolution spline approximation of $g(x) \in L_2$. In particular, we note that $g_m^n(x)$, which is the approximation of $g(x)$ at resolution m, can be entirely determined from $g^n(x)$ since $\mathbf{S}_m^n \subset \mathbf{S}_1^n$. These fundamental results are then used in Section IV for the construction of polynomial spline pyramids.

A. Equivalent B-spline Representations

The classical representation of polynomial splines uses a linear expansion in terms of B-spline basis functions: $\{\beta^n(x-k), k \in \mathbf{Z}\}$ [22]. These functions are shifted replicates of a scaling function $\beta^n(x)$, which has the essential property of having a compact support of minimum size [26]. However, a whole variety of other shift-invariant representations are also

TABLE II
ALTERNATIVE SETS OF BASIS FUNCTIONS OF $\mathbf{S}_1^n$ AND THEIR SPECIFIC PROPERTIES

	Basic	Cardinal	Orthogonal	Dual
Specific Properties	compact support, fast EXPAND	interpolation	orthogonality	fast REDUCE (FIR)
Basis function	$\beta^n(x)$	$\eta^n(x)$	$\phi^n(x)$	$\mathring{\beta}^n(x)$
Weighting coefficients	δ_0 (id.)	$(b^n)^{-1}$	$(b^{2n+1})^{-1/2}$	$(b^{2n+1})^{-1}$
Optimal prefilter	$\mathring{\beta}^n(x)$	$\mathring{\eta}^n(x)$	$\phi^n(x)$	$\beta^n(x)$

conceivable, which is a result that is expressed as follows:

Proposition 1: The set of functions

$$\zeta^n(x) = \sum_{k=-\infty}^{+\infty} p(k)\beta^n(x-k) \tag{3.1}$$

is a basis of $\mathbf{S}_1^n$ provided that p is an invertible convolution operator from l_2 into itself.

The proof of this proposition is rather straightforward and is given in Appendix A for completeness.

Some sets of basis functions are better suited than others depending on the type of computations or interpretations. The basis functions that we have considered are given in Table II. In each case, $g^n(x)$ is entirely characterized by a sequence of discrete coefficients. One such representation is the cardinal expansion for which the expansion coefficients are the sample values of the $g^n(x)$

$$g^n(x) = \sum_{k=-\infty}^{+\infty} g^n(k)\eta^n(x-k) \tag{3.2}$$

and where $\eta^n(x)$ is the so-called cardinal spline function, which has the fundamental interpolation property

$$\forall k \in \mathbf{Z}, \eta^n(k) = \begin{cases} 1 & \text{if } k = 0, \\ 0 & \text{if } k \neq 0. \end{cases} \tag{3.3}$$

Another representation uses orthogonal basis functions that have been introduced recently in the context of the orthogonal wavelet decomposition [13], [14], [33]. These basis functions satisfy the orthogonality condition

$$\forall k \in \mathbf{Z}, \langle \phi^n(x), \phi^n(x-k) \rangle = \begin{cases} 1 & \text{if } k = 0, \\ 0 & \text{if } k \neq 0. \end{cases} \tag{3.4}$$

We will refer to the dual representation, which is also important for our purpose. It is obtained from the last set of basis functions in Table III:

$$g^n(x) = \sum_{k=-\infty}^{+\infty} a(k)\mathring{\beta}^n(x-k) \tag{3.5}$$

where

$$\mathring{\beta}^n(x) = \sum_{k=-\infty}^{+\infty} (b^{2n+1})^{-1}(k)\beta^n(x-k). \tag{3.6}$$

This decomposition has the remarkable property of simplifying certain algorithms, as will be seen later on. Moreover, we

TABLE III
REDUCTION FILTERS FOR THE GENERATION OF POLYNOMIAL SPLINE PYRAMID

Type	Impulse response	Frequency response
Dual	$\frac{1}{2}u_2^n(k)$	$\frac{1}{2}U_2^n(f)=\frac{1}{2^{n+1}}\left(\frac{\sin(2\pi f)}{\sin(\pi f)}\right)^{n+1}$
Basic	$\frac{1}{2}\left[(b^{2n+1})^{-1}\right]_{\uparrow 2} * b^{2n+1} * u_2^n(k)$	$\frac{1}{2}U_2^n(f)\times\left(\frac{B_1^{2n+1}(f)}{B_1^{2n+1}(2f)}\right)$
Orthogonal	$\frac{1}{2}\left[(b^{2n+1})^{-1/2}\right]_{\uparrow 2} * (b^{2n+1})^{1/2} * u_2^n(k)$	$\frac{1}{2}U_2^n(f)\times\sqrt{\frac{B_1^{2n+1}(f)}{B_1^{2n+1}(2f)}}$
Cardinal	$\frac{1}{2}\left[b^n*(b^{2n+1})^{-1}\right]_{\uparrow 2} * (b^n)^{-1} * b^{2n+1} * u_2^n(k)$	$\frac{1}{2}U_2^n(f)\times\left(\frac{B_1^n(2f)\,B_1^{2n+1}(f)}{B_1^n(f)\,B_1^{2n+1}(2f)}\right)$
General	$\frac{1}{2}\left[(\check{p}*b^{2n+1})^{-1}\right]_{\uparrow 2} * p * b^{2n+1} * u_2^n(k)$	$\frac{1}{2}U_2^n(f)\times\left(\frac{P(f)\,B_1^{2n+1}(f)}{\check{P}(2f)\,B_1^{2n+1}(2f)}\right)$

with n odd and $B_1^n(f) = \sum_{k=-\infty}^{+\infty}[\mathrm{sinc}(f-k)]^{n+1} = b^n(0) + \sum_{k=1}^{(n+1)/2} 2b^n(k)\cos(2\pi kf)$.

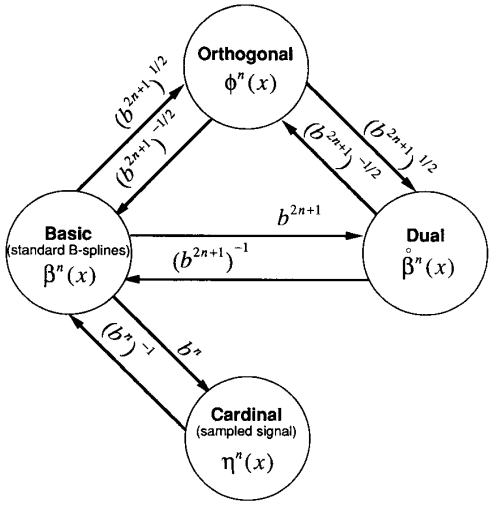

Fig. 1. Digital filters for the conversion between several equivalent polynomial spline representations of signals.

will show that it is closely related to the conventional scale-space representation obtained by convolution of the signal with Gaussian kernels of increasing size [17], [18].

Obviously, expanded versions of these modified basis functions $\zeta_m^n(x) := \zeta^n(x/m)$ can also be used to represent polynomial spline functions at coarser resolution levels: $g_m^n(x) \in \mathbf{S}_m^n$. Moreover, the conversion between one representation and another can be achieved by digital filtering, as schematized in Fig. 1.

B. Least Squares Approximations by Continuous Filtering

We now turn to the issue of determining the multiscale spline decomposition of a function $g(x) \in L_2$. Since all vector spaces $\mathbf{S}_m^n$ are closed subspaces of L_2, the minimum L_2-norm approximation of $g(x)$ is obtained by projecting $g(x)$ into $\mathbf{S}_m^n$. The following theorem suggests a computational procedure to accomplish this task.

Theorem 1: Let $\{\zeta_m^n(x-mk), k \in \boldsymbol{Z}\}$ be a set of shift-invariant basis functions of $\mathbf{S}_m^n$:

$$\zeta_m^n(x) = \sum_{k=-\infty}^{+\infty} p(k)\beta_m^n(x-mk)$$

where p is an invertible symmetrical convolution operator from l_2 into itself. The coefficients $c_m(k)$ of the projection of a function $g \in L_2$ into $\mathbf{S}_m^n$ in the representation

$$g_m^n(x) = \sum_{k=-\infty}^{+\infty} c_m(k)\zeta_m^n(x-mk) \tag{3.7}$$

are given by

$$c_m(k) = \frac{1}{m}\mathring{\zeta}_m^n * g(x)|_{x=mk} \tag{3.8}$$

where the function $\mathring{\zeta}_m^n(x)$ is defined by

$$\mathring{\zeta}_m^n(x) = \sum_{k=-\infty}^{+\infty} (p * b^{2n+1})^{-1}(k)\beta_m^n(x-mk). \tag{3.9}$$

The proof of this theorem for $m = 1$ and $p(k) = \delta_0(k)$ is given in [31] and can be adapted for the present case. The interpretation of this result is that the expansion coefficients are obtained by sampling a continuously filtered signal (see (3.8)). The prefilter, whose impulse response is $\mathring{\zeta}_m^n(x)$, has a role that is very similar to an anti-aliasing filter used in conventional sampling theory [31]. Likewise, the function $\zeta_m^n(x)$ represents the impulse response of an interpolator that can be applied in a post-filtering phase to reconstruct $g_m^n(x)$. It can be verified that the functions $\mathring{\zeta}_m^n(x)$ and $\zeta_m^n(x)$ are biorthogonal. The prefiltering functions for the spline representations considered in Section III-A are also given in Table II. A distinctive feature of the orthogonal representation is that the prefilter and basis functions are identical. The basic and dual representations are complementary in the sense that the prefilter and basis functions are simply interchanged. The corresponding pairs of functions for a cubic spline representation are shown in Fig. 2. A graph of the frequency responses of these filters can be found in [31].

The computational procedure suggested by Theorem 1 is simplified if the signal is first prefiltered with a normalized expanded B-spline and sampled thereafter:

$$a_m(k) = \frac{1}{m}\beta_m^n * g(x)|_{x=mk} \tag{3.10}$$

It is straightforward to show that the expansion coefficients in (3.7) can then be determined by digital filtering:

$$c_m(k) = (p)^{-1} * (b^{2n+1})^{-1} * a_m(k) \tag{3.11}$$

which simplifies the implementation of the continuous filter defined by (3.9). Since the optimal prefilter associated with $\mathring{\beta}_m^n(x)$ is $\beta_m^n(x)$, the use of the dual representation

$$g_m^n(x) = \sum_{k=-\infty}^{+\infty} a_m(k)\mathring{\beta}_m^n(x-mk) \tag{3.12}$$

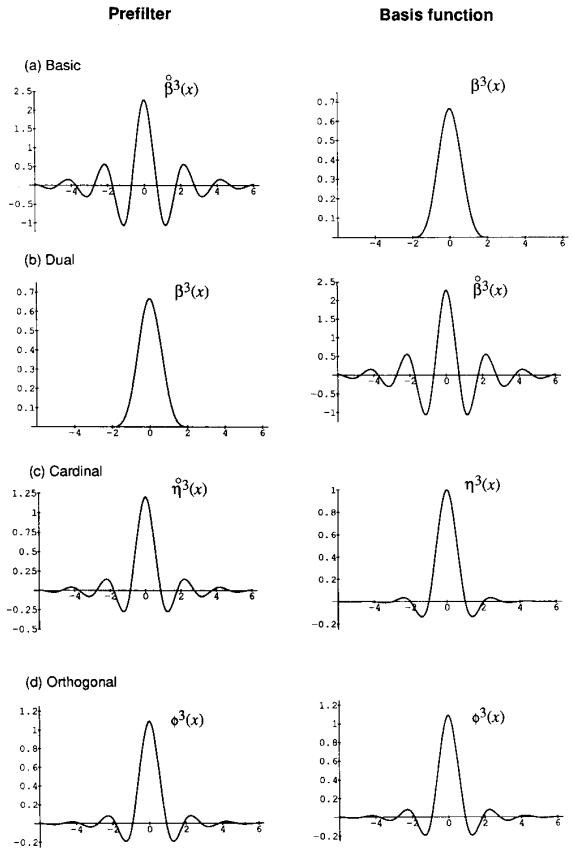

Fig. 2. Optimal prefilters and basis functions for four equivalent representation of cubic spline polynomial approximations.

where $a_m(k)$ is defined by (3.10) has the advantage of avoiding the extra convolution step in (3.11). The coefficients $a_m(k)$ are obtained by sampling the result of the convolution between $g(x)$ and $\beta_m^n(x)/m$. The convolution kernel $\beta_m^n(x)/m$ is a positive function with a unit integral (a property of probability density functions) and a variance that is equal to $m(n+1)/12$. For increasing values of n, the functions $\beta_m^n(x)/m$ tend to be increasingly Gaussian like. In fact, the resemblance with a Gaussian pulse is already striking for values of n as low as 2 and 3 (cf. Fig. 1(c)-(d) in [25]); the integrated rms errors for Gaussian approximations of equal variance are 3.58 and 2.38%, respectively. This procedure is therefore very similar to the Gaussian convolution approach described by Witkin [17], although the present interpretation of the samples is quite different.

Finally, we note that the additional convolutions in (3.11) can be interpreted as two successive changes of coordinate system; $(b^{2n+1})^{-1}$ performs the conversion from dual to basic representation (cf. Fig. 1) and $(p)^{-1}$ from basic to generic, as specified in Proposition 1.

C. Least Squares Approximation by Digital Filtering

The procedure suggested by Theorem 1 is not very practical since it involves the processing of a continuous function $g(x)$. Since $\mathbf{S}_m^n \subset \mathbf{S}_1^n$ (assuming that m and n are not both even), we can expect that $g_m^n(x)$ is entirely specified from the expansion coefficients of $g^n(x) \in \mathbf{S}_1^n$. This is essentially due to the fact that $\beta_m^n(x) \in \mathbf{S}_1^n$, which is also equivalent to saying that the expanded B-spline can be represented as a weighted sum of finer B-splines:

$$\beta_m^n(x) = \sum_{k=-\infty}^{+\infty} u_m^n(k)\beta^n(x-k). \tag{3.13}$$

We note that this expression follows directly from (2.7). By using this result, we get the following theorem, which provides a solution to the general L_2 approximation problem.

Theorem 2: Let $\{\zeta_1^n(x-k), k \in \mathbf{Z}\}$ and $\{\check{\zeta}_m^n(x-mk), k \in \mathbf{Z}\}$ be two sets of shift-invariant basis functions of $\mathbf{S}_1^n$ and $\mathbf{S}_m^n$, respectively. $\zeta_1^n(x)$ and $\check{\zeta}_m^n(x)$ are represented as

$$\zeta_1^n(x) = \sum_{k=-\infty}^{+\infty} p(k)\beta^n(x-k)$$

$$\check{\zeta}_m^n(x) = \sum_{k=-\infty}^{+\infty} \check{p}(k)\beta_m^n(x-mk)$$

where p and $\check{p}$ are invertible convolution operators. The orthogonal projection of the function $g_1^n(x) \in \mathbf{S}_1^n$

$$g_1^n(x) = \sum_{k=-\infty}^{+\infty} c_1(k)\zeta_1^n(x-k) \tag{3.14}$$

into $\mathbf{S}_m^n$ is given by

$$g_m^n(x) = \sum_{k=-\infty}^{+\infty} \check{c}_m(k)\check{\zeta}_m^n(x-mk) \tag{3.15}$$

where the expansion coefficients $\check{c}_m(k)$ are obtained as

$$\check{c}_m(k) = \frac{1}{m}(\check{p}*b^{2n+1})^{-1}*[p*b^{2n+1}*u_m^n*c_1]_{\downarrow m}(k). \tag{3.16}$$

The proof is given in Appendix B. The same algorithm is also applicable for the projection of $g_i^n(x) \in \mathbf{S}_i^n$ into $\mathbf{S}_{im}^n$, where i and m are some positive integers.

As in the previous case, we note that this procedure is greatly simplified if we choose $p = \check{p} = (b^{2n+1})^{-1}$. The corresponding representation of $g_1^n(x)$ is the one described by (3.5), and its projection into $\mathbf{S}_m^n$ is given by (3.12) with

$$a_m(k) = \frac{1}{m}[u_m^n * a_1]_{\downarrow m}(k) \tag{3.17}$$

where $u_m^n(k)$ is the impulse response of the finite impulse response (FIR) filter described by (2.8).

IV. Polynomial Spline Pyramids

A. Definition

A polynomial spline pyramid is a multiresolution transform of a signal $g(x) \in L_2$, which satisfies the general definition given by Mallat [14]. More specifically, it is obtained from a sequence of approximations $\{g_{(i)}^n(x) \in \mathbf{S}_{2^i}^n, i \in \mathbf{Z}\}$ with the property that the integrated square error (L_2 norm) between

$g(x)$ and any of those functions is minimum. Only a few resolution levels of this decomposition need to be determined in practice. By convention, the initial spacing between the knot points of the spline approximation is chosen to be one. This spacing is then increased by a factor of two at each iteration, and the process is stopped at a certain resolution level K. The determination of this transform proceeds by repeated projection of $g(x)$ onto a sequence of embedded subspaces of L_2: $\mathbf{S}_1^n \supset \mathbf{S}_2^n \cdots \supset \mathbf{S}_{2^i}^n \cdots \supset \mathbf{S}_{2^K}^n$, where it is, from now on, implicitly assumed that n is odd. The spline approximations $g_{(i)}^n(x), i = 0, \cdots, K$ are entirely specified in terms of their expansion coefficients. The sequence of these coefficients leads to a discrete pyramidal representation with a number of samples that is decreased by a factor of two at each iteration. The present formulation differs from the one presented by Mallat in that it considers a characterization of the approximation functions using basis functions that are not necessarily orthogonal.

B. A Simple Algorithm

We first describe a simple computational procedure that takes advantage of the simplifications that occur when the multiresolution approximations are represented as

$$g_{(i)}^n(x) = \sum_{k=-\infty}^{+\infty} a_{(i)}(k)\mathring{\beta}_{2^i}^n(x - 2^i k) \tag{4.1}$$

where the scaling function $\mathring{\beta}^n(x)$ is defined by (3.6).

To initialize the procedure, we have to distinguish between two cases, depending on whether the input of the system is a continuous function or a sequence of discrete sample values. In the first case, the use of Theorem 1 yields

$$a_{(0)}(k) = (\beta^n * g)(x)|_{x=k} \qquad \forall k \in \mathbf{Z} \tag{4.2}$$

which indicates that the input of the system $g(x)$ has to be prefiltered with a basic B-spline prior to sampling. The principle of this approximation is further discussed in [31]. If, on the other hand, the input is a sequence of discrete values $g(k) \in l_2$, we use the cardinal representation to determine a spline that precisely interpolates $g(k)$:

$$g_{(0)}^n(k) = g(k) \qquad \forall k \in \mathbf{Z}. \tag{4.3}$$

To determine the coefficients of the dual representation (4.1), this sequence is filtered as

$$a_{(0)}(k) = b^{2n+1} * (b^n)^{-1} * g_{(0)}^n(k) \qquad \forall k \in \mathbf{Z} \tag{4.4}$$

which is equivalent to performing two successive changes of coordinate system (cf. Fig. 1). We note that b^{2n+1} is the response of a simple FIR filter. The convolution with $(b^n)^{-1}$ can be performed using the recursive algorithm described in [25].

By making use of Theorem 2, we find that the expansion coefficients of the subsequent approximations for $(i = 1, \cdots, K)$ can be determined recursively as

$$a_{(i)}(k) = \frac{1}{2}[u_2^n * a_{(i-1)}]_{\downarrow 2}(k) \qquad \forall k \in \mathbf{Z}. \tag{4.5}$$

This defines the basic REDUCE operation. The operator u_2^n corresponds to a simple FIR filter. By using (2.8), we can show that the corresponding filter coefficients are the binomial coefficients:

$$u_2^n(k) = \begin{cases} \dfrac{1}{2^n}\binom{n+1}{k+(n+1)/2}, & |k| \le (n+1)/2 \\ 0 & \text{otherwise.} \end{cases} \tag{4.6}$$

Since this filter can be decomposed into a cascade of moving average filters, we can use the central limit theorem [34] to show that $u_2^n(k)$ converges to a Gaussian for increasing values of n. A simple expression for its frequency response is

$$U_2^n(e^{j2\pi f}) = \frac{1}{2^n}\left(\frac{\sin(2\pi f)}{\sin(\pi f)}\right)^{n+1} = 2\cos^{n+1}(\pi f). \tag{4.7}$$

Another consequence of this property is that the convolution in (4.5) can be implemented using additions only, plus a final (optional) normalization by 2^{n+1}.

The complement of REDUCE is the EXPAND function that maps a coarser level of pyramid onto a finer grid. This process is equivalent to a polynomial spline interpolation and is the simplest to perform for an expansion in term of standard B-splines [25]. For a given level of the pyramid (i_o), the conversion from dual to basic B-spline basis is obtained by digital filtering:

$$c_{(i_o,i_o)}(k) := c_{(i_o)}(k) = (b^{2n+1})^{-1} * a_{(i_o)}(k). \tag{4.8}$$

It is the initialization part of the procedure. Let $c_{(i_o,i)}(k)$, where $i_o \ge i$, denote the extrapolation at resolution (i) associated with the coarser level (i_o) of the pyramid. By using (3.13), it is not difficult to show that $c_{(i_o,i)}(k)$ can be determined by recursive application of the EXPAND function defined as

$$c_{(i_o,j)}(k) = u_2^n * [c_{(i_o,j+1)}]_{\uparrow 2}(k) \tag{4.9}$$

where j is decremented from $i_o + 1$ down to i. Finally, if desired, the corresponding image interpolation $g_{(i_o,i)}^n(k) := g_{(i_o)}^n(2^i k)$ at resolution (i) is determined by FIR post-filtering

$$g_{(i_o,i)}^n(k) = b^n * c_{(i_o,i)}(k). \tag{4.10}$$

The whole algorithmic procedure is schematically represented in Fig. 3. In this representation, we have assumed that the input of the system is a discrete sequence of data points. We note the striking duality between the REDUCE and EXPAND functions. In this implementation, the REDUCE and EXPAND filters are FIR binomial operators (cf. (4.6)). We also note that for $n = 3$, the EXPAND and REDUCE functions are almost identical to the functions proposed by Burt for the generation of the Gaussian or Laplacian pyramid [9], [15] (c.f. discussion below). The major difference, however, is our requirement for an initialization sequence that performs a change of coordinates and involves an additional level of digital filtering.

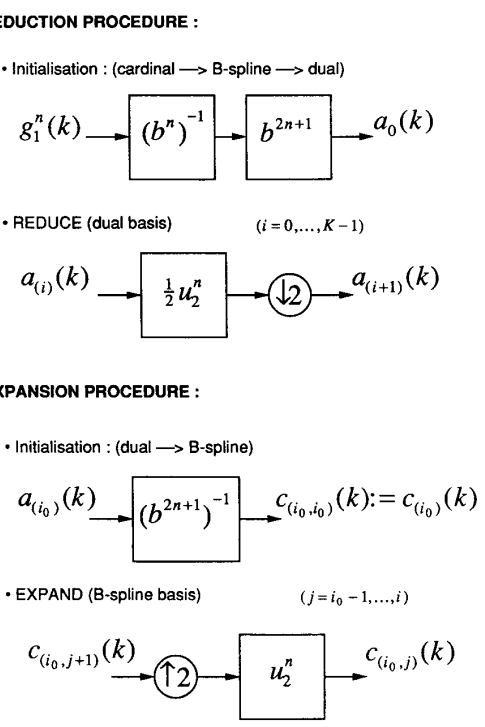

Fig. 3. Schematic representation of the simplified REDUCE (dual representation) and EXPAND (basic representation) procedures associated with the L_2-spline pyramid.

C. Generalized EXPAND and REDUCE Functions

The reduced expansion coefficients in (4.5) are obtained by filtering and decimation by a factor of two. The same procedure is also applicable for other representations, but the filters tend to be more complex. Let us consider the general spline representation

$$g_{(i)}^n(x) = \sum_{k=-\infty}^{+\infty} c_{(i)}(k)\zeta_{2^i}^n(x - 2^i k))$$

$$g_{(i+1)}^n(x) = \sum_{k=-\infty}^{+\infty} \check{c}_{(i+1)}(k)\check{\zeta}_{2^{i+1}}^n(x - 2^{i+1}k)$$

where $\zeta_{2^i}^n(x)$ and $\check{\zeta}_{2^{i+1}}^n(x)$ are defined as in Theorem 2. By using Theorem 2, it is not difficult to show that the sequences of $c_{(i)}$'s can be computed iteratively as

$$\check{c}_{(i+1)}(k) := \text{REDUCE}(c_{(i)}) = [v * c_{(i)}]_{\downarrow 2}(k) \tag{4.11}$$

where the reduction filter v is

$$v(k) = \frac{1}{2}[(\check{p} * b^{2n+1})^{-1}]_{\uparrow 2} * p * b^{2n+1} * u_2^n(k). \tag{4.12}$$

This is the most general form of the REDUCE operation. The last expression was used to determine the filters for all spline representations considered in Section III-A, and the corresponding impulse and frequency responses are given in Table III.

Likewise, the coefficients of an expanded version of the signal in (4.9) are obtained by upsampling by a factor of two and post-filtering; this is a procedure that can be readily extended to other spline representations.

Let us consider the signal associated with the coarser representation at resolution level $(i+1)$. Since $\mathbf{S}_{2^{i+1}}^n \subset \mathbf{S}_{2^i}^n$, the same signal can also be represented using basis functions at the finer resolution level (i):

$$g_{(i+1)}^n(x) = \sum_{k=-\infty}^{+\infty} \check{c}_{(i+1)}(k)\check{\zeta}_{2^{i+1}}^n(x - 2^{i+1}k)$$

$$= \sum_{k=-\infty}^{+\infty} c_{(i+1,i)}(k)\zeta_{2^i}^n(x - 2^i k) \tag{4.13}$$

where the basis functions $\zeta_{2^i}^n(x)$ and $\check{\zeta}_{2^{i+1}}^n(x)$ are defined as previously. The question now is how to determine the finer sequence of coefficients $c_{(i+1,i)}(k)$ from $\check{c}_{(i+1)}(k)$. By using (3.13) and making the suitable changes of coordinate system, we find that

$$c_{(i+1,i)}(k) := \text{EXPAND}(\check{c}_{(i+1)}) = w * [\check{c}_{(i+1)}]_{\uparrow 2}(k) \tag{4.14}$$

where

$$w(k) = [\check{p}]_{\uparrow 2} * (p)^{-1} * u_2^n(k) \tag{4.15}$$

which is the corresponding generalized form of the EXPAND function. This process can be iterated in order to compute image interpolations or representations at any finer resolution level. The general form of the impulse and frequency response of w for the various polynomial spline representations considered in this paper is given in Table IV.

We note that all filters in Tables III and IV, with the notable exception of u_2^n, have an infinite impulse response (IIR). Most of these can be implemented recursively. In practice, however, we have found it preferable to use the procedure described in the previous section and to derive alternative representations when they are needed using the conversion rules schematized in Fig. 1.

A case that stands apart is the representation that uses orthogonal basis functions. The corresponding square-root filters cannot be implemented recursively. However, this decomposition has the advantage that the reduction and expansion filters are identical (cf. the third row in Tables III and IV). The recommended filter implementation in this case is a truncated FIR approximation. The filter coefficients can be determined by discretizing the frequency response given in Table III and performing the inverse discrete Fourier transform. This approach has been taken by Mallat for the design of the filter for the orthogonal cubic spline pyramid (see table 1 in Appendix A of [14]). In this respect, we note that the frequency responses of the filters associated with the orthogonal transformations given in Tables III or IV are alternative but equivalent forms of (57) and (58) in [14]. What may be an advantage of the present form of these equations is that they allows us to compute the frequency responses directly by substituting the appropriate expression of $B_1^n(f)$ (which are easily derived from Table I or (2.2) and (2.5)) without having to deal explicitly with the evaluation of infinite sums.

TABLE IV
EXPANSION FILTER FOR THE POLYNOMIAL SPLINE PYRAMIDS WITH n ODD

Type	Impulse response	Frequency response
Dual	$[(b^{2n+1})^{-1}]_{\uparrow 2} * b^{2n+1} * u_2^n(k)$	$U_2^n(f) \times \left(\frac{B_1^{2n+1}(f)}{B_1^{2n+1}(2f)}\right)$
Basic	$u_2^n(k)$	$U_2^n(f) = \frac{1}{2^n}\left(\frac{\sin(2\pi f)}{\sin(\pi f)}\right)^{n+1}$
Orthogonal	$[(b^{2n+1})^{-1/2}]_{\uparrow 2} * (b^{2n+1})^{1/2} * u_2^n(k)$	$U_2^n(f) \times \sqrt{\frac{B_1^{2n+1}(f)}{B_1^{2n+1}(2f)}}$
Cardinal	$[(b^n)^{-1}]_{\uparrow 2} * b^n * u_2^n(k)$	$U_2^n(f) \times \left(\frac{B_1^n(f)}{B_1^n(2f)}\right)$
General	$[\check{P}]_{\uparrow 2} * (p)^{-1} * u_2^n(k)$	$U_2^n(f) \times \left(\frac{\check{P}(2f)}{P(f)}\right)$

D. The Difference (or Laplacian) Pyramid

During an iteration, $g_{(i)}^n(x)$ is approximated by $g_{(i+1)}^n(x)$. The loss of information is measured by the residual error

$$\varepsilon_{(i+1,i)}(x) = g_{(i)}^n(x) - g_{(i+1)}^n(x). \tag{4.16}$$

We know that $\varepsilon_{(i+1,i)}(x) \in \mathbf{S}_{2^i}^n$ since $g_{(i)}^n(x) \in \mathbf{S}_{2^i}^n$ and $g_{(i+1)}^n(x) \in \mathbf{S}_{2^{i+1}}^n \subset \mathbf{S}_{2^i}^n$. It follows that $\varepsilon_{(i+1,i)}(x)$ is entirely characterized by its spline coefficients at resolution 2^i, which, due to the linearity of the expansion, are given by

$$\Delta c_{(i+1,i)}(k) = c_{(i+1)}(k) - c_{(i+1,i)}(k) \tag{4.17}$$

where $c_{(i+1,i)}(k) = \text{EXPAND}(c_{(i)})$ (cf. (4.14) and (4.15)). We note, however, that this representation has twice as many coefficients as necessary. In 2-D, this representation is overcomplete by a factor of 4/3. A more compact representation can be obtained by using wavelet functions similar to those defined by Mallat and Lemarié [14], [33]; this issue will be addressed in greater detail in a forthcoming paper [35].

The loss of information is well visualized in terms of its samples (cardinal B-spline representation): $\Delta g_{(i+1,i)}(k) := \varepsilon_{(i+1,i)}(2^i k)$. The sequence of error images for $i = 0, \cdots, K-1$ can be displayed in the spline difference pyramid, which is a data structure that is very similar to the one described by Burt [9]. From our previous results, we know that this data structure is particularly easy to construct from a standard representation using basic B-spline coefficients:

$$\Delta g_{(i+1,i)}(k) := b^n * (c_{(i)}(k) - u_2^n * [c_{(i+1)}]_{\uparrow 2}(k)). \tag{4.18}$$

V. RESULTS AND DISCUSSIONS

In this section, we present some experimental examples using 2-D images. We then discuss some of the implications of our results and the way the present approach relates to several multiresolution methods described in the literature.

A. Experimental Results

All algorithms were coded in FORTRAN on a low-end workstation (standard 16-Mhz Apple Macintosh IIcx). The basic spline pyramid was implemented using a straightforward separable extension of the procedure schematized in Fig. 3.

Fig. 4. Cardinal representation of the L_2 cubic spline pyramid (sampled image values): (0): original 208 × 222 "Lena" image. Levels (1) to (4) computed from images (1)-(4) in Fig. 6 by successive row and column filtering with b^3 (separable indirect B-spline filter of order 3).

All inverse filters were implemented recursively from a cascade of simple causal and anticausal exponential filters [25]. Although all images were stored in short integer format to reduce memory space, the intermediate results of 1-D filtering along a row or a column were stored in a real vector to prevent the propagation of round-off errors. The bilinear and cubic spline orthogonal pyramids were implemented using FIR approximations of length 13 and 23, respectively. For the latter case, we found our filter design to be consistent with the one reported in Table I of Appendix B of [14] with the exception of the sign of coefficients $h(5)$ and $h(6)$, which should be interchanged.

Another important practical issue is the specification of boundary conditions since the signals encountered in practice have a finite extend. For practical convenience and to avoid discontinuities, the signals at the finer level were extended on both sides by using their mirror image, which is a standard practice in image processing. Compatible boundary conditions were used at the coarser resolution levels.

To illustrate the concepts described in the previous section, we first present some examples of polynomial spline pyramids for $n = 3$ (cubic splines). The original test image is shown in Fig. 4 at resolution level (0). The cubic spline pyramid was computed using the dual representation. The initial image was first prefiltered (initialization procedure) to obtain level (0) in Fig. 5, which is a slightly blurred version of the original image. The frequency response of this filter, which slightly attenuates higher spatial frequencies, is provided by the lower curve in Fig. 7. The remaining levels of the pyramid were obtained by successive low-pass filtering and decimation along the rows and columns using the binomial kernel $u_2^3(k)$ of length 5 (cf. Table I). The resulting image pyramid is shown in Fig. 5, with all levels appearing as somewhat smoothed copies of the original image. We note that this representation is extremely similar to the commonly used Gaussian pyramid proposed by Burt [9], [15]; the only difference is the use of a prefilter in the initialization phase to determine level (0) so that in our case, it is different from the original image. The corresponding cardinal (Fig. 4) and basic B-spline pyramids (Fig. 6) can be

Fig. 5. Dual representation of the L_2 cubic spline pyramid. This image pyramid was computed using the simplified REDUCE procedure schematized in Fig. 3.

Fig. 6. Basic representation of the L_2 cubic spline pyramid (standard B-spline coefficients). Levels (0) to (4) computed from images (0)-(4) in Fig. 5 by successive row and column filtering with $(b^7)^{-1}$ (separable direct B-spline filter of order 7).

determined from the dual representation by digital filtering of each level using the conversion rules given in Fig. 2. The basic representation has the property of enhancing high frequencies, which is a fact that has been pointed out previously [25]. No such distortion occurs for the cardinal representation because it preserves the original image at level (0). In terms of fidelity of the representation, this decomposition is visually the most satisfactory one. It also stands between the dual and basic representations, which have the tendency to enhance lower or higher spatial frequencies, respectively. This qualitative observation is supported quantitatively by the analysis of the frequency responses of the conversion filters between the sampled (cardinal) and the other representations (cf. Fig. 7). The orthogonal pyramid, which is not shown here, is almost indistinguishable from the cardinal representation since the conversion filter is essentially an all-pass filter with the exception of a slight attenuation of higher frequencies.

A visual display of the loss of information that occurs during resolution conversion is provided by the difference pyramid described in Section IV-C. Fig. 8 provides a comparison between this data structure for $n = 3$ and Burt's

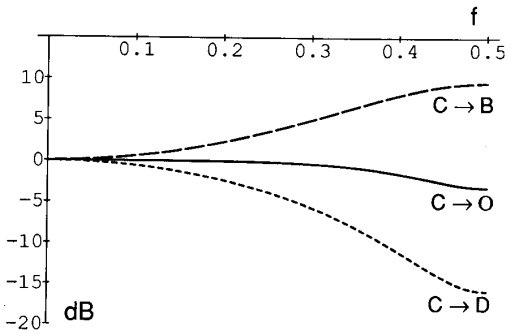

Fig. 7. Frequency responses of the conversion filters from cardinal to orthogonal, dual, and basic spline representations for $n = 3$ (cubic splines).

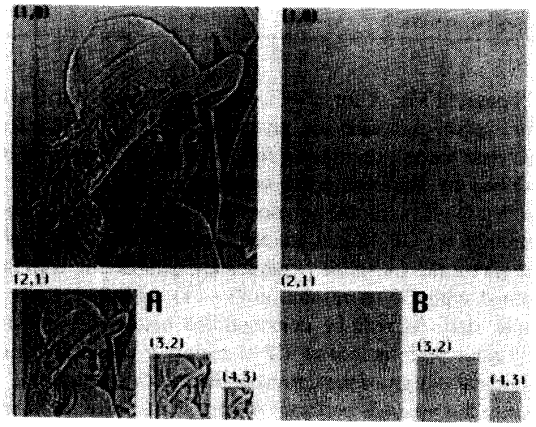

Fig. 8. Comparison between the Burt's Laplacian pyramid (a) and the cardinal representation of the difference cubic spline pyramid (b).

Laplacian pyramid with a parameter value of $a = 3/8$ [9]. The same intensity scaling factors were applied to all images to facilitate the comparison. For Burt's Laplacian pyramid, the amount of information displayed at each resolution level is not insignificant, and the main subject is still readily recognizable. In the case of the cubic spline pyramid, the energy of the Laplacian is reduced drastically, and only very high-frequency details are visible in this representation.

The quality of the image approximation associated with a given level of the polynomial spline pyramid can be assessed using a standard measure of the signal-to-noise ratio (SNR) in decibels:

$$\mathrm{SNR}_{(i,0)} = 10 \log_{10} \left(\frac{(g_{\max} - g_{\min})^2}{\frac{1}{KL} \sum_{k=1}^{K} \sum_{l=1}^{L} (\Delta g_{(i,0)}(k,l))^2} \right). \tag{5.1}$$

The quantities $g_{\max}$ and $g_{\min}$ refer to the maximum and minimum gray level values of the $K \times L$ reference image, and $\Delta g_{(i,0)}(k,l)$ denotes the error between the original image and the full-resolution approximation (cardinal representation) obtained from resolution level (i) of the pyramid. The image pyramid can be stored in any of the forms described previously since all these data structures are equivalent representations of the same information. The results of these computations for the

TABLE V
COMPARISON OF IMAGE PYRAMIDS IN TERMS OF THE SIGNAL-TO-NOISE RATIO ASSOCIATED WITH THE DIFFERENT LEVELS FOR THE TEST IMAGE IN FIG. 4

Pyramid	level 1	level 2	level 3	level 4
L_2 spline (n=1)	27.55 dB	22.59 dB	19.21 dB	16.19 dB
L_2 spline (n=3)	28.64 dB	23.02 dB	19.51 dB	16.43 dB
Gaussian (Burt)	23.70 dB	19.44 dB	16.48 dB	14.21 dB
Orthogonal (n=1) with no conversion	27.46 dB	22.40 dB	19.01 dB	16.06 dB
Orthogonal (n=3) with no conversion	28.59 dB	22.97 dB	19.47 dB	16.41 dB
Dual (n=3) with no conversion	28.60 dB	22.95 dB	19.47 dB	16.40 dB

test image in Fig. 4 for $n = 1$ (bilinear pyramid) and $n = 3$ (cubic spline pyramid) are given in Table V. We have also performed these experiments for the Gaussian pyramid (GP) described by Burt using the same parameter as before. We note that in all cases, the polynomial spline pyramids performs better than the GP. In fact, the SNR values obtained at a given level (i) for the L_2 spline pyramids are comparable with those obtained with GP at resolution $(i - 1)$ with four times the sample size. As will be demonstrated below, the comparatively poor performance of GP is mainly a consequence of a suboptimal design of the corresponding EXPAND function. The cubic spline pyramid performs slightly better than the bilinear pyramid, which is a result that is not surprising given the better smoothness properties of the approximations of the former. Similar results have been obtained with all other images to which we have applied the procedure.

We have already pointed out that the orthogonal representation is extremely close to the cardinal one. It therefore appears legitimate to substitute the initial pixel values for the orthogonal spline coefficients at level 0 and vice versa. However, while doing so, one has to be aware of the fact that the underlying continuous signal that one is approximating is not the same as before in the sense that it does not interpolate the pixel values of the image precisely. The main advantage is that one avoids the use of pre and postfilters for the conversion from and to cardinal representation while the procedure is still coherent. We note that this approach has been taken implicitly by Mallat for his experiments with the wavelet transform [14]. The SNR values obtained in this case are also given in Table V and can be seen to be only very slightly below those obtained with the previous approach. In fact, the same strategy can also be used for the dual representation, which essentially amounts to using Burt's method of constructing the Gaussian pyramid with the modified EXPAND function specified by the first line in Table IV with $n = 3$. Here too, the results are virtually undistinguishable from those obtained with the L_2 cubic spline pyramid, and the improvement over Burt's initial scheme is quite significant. It is important to keep in mind, however, that the underlying continuous signals used in these different experiments are not the same, which also means that the approximations computed in each case are not equivalent.

B. Discussion

1) Equivalent Polynomial Spline Pyramid Representations: An important point that has been emphasized all along the presentation is the availability of a variety of equivalent polynomial spline representations (cf. Proposition 1). These representations are associated with different sets of shift-invariant basis functions but are all equivalent characterizations of the underlying continuous signal approximations. The conversion between any two of these representations (change of coordinate system) occurs by digital filtering, which is a particular form of linear transformation (cf. Fig. 1). Four such representations have been considered in more detail because of their distinctive properties. For instance, the dual representation is associated with the simplest REDUCE filtering operator (binomial filter), which facilitates the generation of the polynomial spline pyramid. This decomposition, which tends to emphasize lower spatial frequencies, is also the one that is the most similar to other frequently used approaches, such as scale-space filtering [17] and the Gaussian pyramid [9]. The standard B-spline representation is associated with the simplest possible form of the EXPAND function and therefore simplifies image interpolation and zooming. It is also especially suited for signal analyses involving operations such as differentiation, integration, searching for extrema, etc$\cdots$, which are well expressed in terms of B-spline coefficients [36]. The cardinal representation is the one that provides the best rendition (i.e., precise sampling) of the underlying continuous signals. From this perspective, it appears to be the most appropriate for conventional digital signal processing. Finally, the orthogonal representation has the remarkable property of using identical REDUCE and EXPAND operators. Moreover, it preserves L_2-norms, meaning that the square integral of the difference between two continuous signal approximations is equal to the sum of squares of the difference between the corresponding coefficients of the orthogonal representation.

2) Interpolation Versus Extrapolation: The EXPAND function provides a general mechanism for extrapolating any of the spline representations that have been considered at a finer resolution level. We have intentionally used the term extrapolation to distinguish between this operation and an interpolation. By interpolation, it is usually meant that the signal values at the grid points are preserved; this is generally not the case for the operation described by (4.14). In effect, a true interpolation occurs only when the cardinal representation of the pyramid is used. This property is a consequence of the vanishing of the underlying basis functions $\eta^n(x)$ at all nonzero integer values (cf. (3.3)), which is a feature that these functions share with $\mathrm{sinc}(x)$—the classical interpolation kernel for bandlimited functions. We can also see from Fig. 2(d) that the orthogonal basis functions for cubic splines differ very slightly from a true interpolator. In practice, this means that the coefficients of the orthogonal representation will be very close numerically to the sampled values of the underlying continuous signal approximation. The observation is also supported

by examination of the frequency response of the conversion filter between cardinal and orthogonal representations, which indicates that these representations only differ very slightly in their higher frequency content. Thus, it appears justifiable to substitute any of these representations for the other, provided that one is aware of the approximations that are involved. From these considerations, we can also conclude that the l_2-norm of the cardinal representation provides a good approximation of the L_2-norm of the interpolating signal; this is not surprising since the former provides a Riemann sum approximation of the integral in the latter.

3) Implementation Considerations: Some of the filters required for the construction of polynomial spline pyramids are simple indirect-spline or binomial FIR kernels, whereas others are IIR (cf. Table I). Most of the IIR operators, with the exception of the filters for the orthogonal representation, can be implemented exactly using the recursive algorithms described in [25]. We note, however, that for image processing applications where the intensity values are typically quantified with 256 gray levels, the use of truncated FIR approximations with a limited number of coefficients is usually acceptable; the only requirement is that the truncation error be below the required level of precision. In terms of efficiency, the selection of a given implementation depends strongly on the configuration of the image processor. For our low-cost Macintosh II image processing workstation, we found the recursive implementation to be the most suitable. In the case of an orthogonal representation, one has no choice but to opt for an FIR approximation. Fortunately, the corresponding impulse response tends to decay rapidly, and a 15- to 20-point FIR approximation seems to be sufficient for most image processing applications. Moreover, the same filter can be used for the REDUCE and EXPAND operations. It also appears from Fig. 2 that the orthogonal representation offers a sort of compromise in terms of localization for both the prefilter and basis functions, which is a property that translates into a relatively fast decay of the impulse response of the corresponding digital filters.

4) Link with Other Approaches: The close similarity between the present signal analysis and a variety of other methods has already been brought into prominence at various stages of the presentation. The dual polynomial spline representation introduced in Section III is especially useful in bringing out such relations. The analogy with the scale-space analysis by Gaussian filtering [17], [18] stems from the fact that B-spline functions are Gaussian-like kernels, especially for higher order splines. This property follows from the well-known convolution property of B-spline functions [29]

$$\beta^n(x) = \underbrace{\beta^0 * \beta^0 * \cdots * \beta^0}_{n+1\text{times}}(x) \tag{5.2}$$

and is a consequence of the central limit theorem, which states that the repeated convolution of any given probability density function with bounded mean and variance (in our case $\beta^0(x)$) converges to a Gaussian [34].

The close relationship with the method proposed by Burt is striking and is especially satisfactory, given that the justification for this latter approach is largely empirical. To be more specific, we recall that the Gaussian-like kernel used by Burt for the generation of the Gaussian or Laplacian pyramids has the following z-transform representation:

$$W(z;a) = \left(\frac{1}{2} - a\right)(z^{-2} + z^2) + \frac{1}{2}(z^{-1} + z) + 2a \tag{5.3}$$

where a is an adjustable parameter. For $a = 3/8 = 0.375$, this filter is equivalent to the operator $U_2^3(z)$ (cf. Table I) used in the generation of the cubic spline pyramid by the dual representation. This particular choice of a is close to the value 0.36 recommended by Burt for greatest reduction of the side lobes of the transfer function [15]. Moreover, we have another equivalence for $a = 1/2$, in which case, Burt's operator is identical to $U_2^1(z)$ and corresponds to a first-order spline interpolator. This particularly simple weighting kernel is also used frequently in the implementation of multigrid methods [4].

Another point is that the filters used in the generation of the dual spline pyramid fall into the class of generalized binomial kernels considered by Lindeberg [21]. Since sampling does not introduce any new local extrema, we can use the theoretical results of Lindeberg to show that the dual representation is a valid discrete scale-space representation in the sense that the occurrence of new minima or maxima at lower resolution levels is prohibited. This particular feature can be interpreted as a "structure preserving" property. The spline pyramid also satisfies a causality principle in the sense that a coarser level is entirely determined from any finer resolution level. These properties are very similar to those associated with the Gaussian kernel in conventional scale-space filtering (i.e., causality, shift invariance, and structure preservation) [19].

Finally, we note that the polynomial spline approximation problem can also be formulated in a purely discrete framework replacing continuous functions by discrete signals. In this case, the basis functions are discrete, and the minimization uses the discrete l_2-norm [37]. The corresponding discrete cardinal spline filters are slightly different from those derived in the present study, but these differences get smaller for coarser-level approximations.

5) Consistent REDUCE and EXPAND Functions: An important aspect of the present formulation is to provide a consistent design for the REDUCE and EXPAND functions to minimize information loss during resolution conversion, which is a feature that is not shared by many of the approaches discussed previously. We have shown that the optimal REDUCE and EXPAND filtering operators are generally not identical unless the underlying basis functions are orthogonal, precisely, the case in the construction method proposed by Mallat [14]. The fact that an EXPAND function of the type described by Burt is not optimal has been illustrated by Fig. 8. Our theoretical results also suggest two simple ways to correct for this limitation. The first is to choose as EXPAND operator the true complement of a given REDUCE function (cf. Tables III and IV) that is associated with the same basis functions. The second solution is to perform a change of coordinate system and to expand the image in the basic B-spline representation, which is the approach we have taken for most of our experiments. We conjecture that the use of these techniques could significantly

improve the performance of the coding scheme described in [9]. These modifications may also be useful to improve the rates of convergence of some multigrid procedures.

Based on its excellent data-reduction properties, the polynomial spline pyramid should provide an attractive alternative to the standard Gaussian (or Laplacian) pyramid that is commonly used in image processing and computer vision. This representation may therefore be potentially useful in applications such as image segmentation [38], edge detection [39], feature extraction [15], and a variety of computer vision problems that are best formulated in a continuous framework and may benefit from a multiresolution implementation [5], [7], [30].

6) Link with Conventional Sampling Theory: The standard signal processing approach for sampling rate conversion is dictated by Shannon's sampling theorem [40]. The data sequence is first bandlimited by prefiltering with an ideal low-pass filter and down-sampled thereafter. This band-limited signal may be reconstructed without any loss from its samples by upsampling and postfiltering with the same low-pass filter that implements an ideal sinc interpolator [41]. We note that the pre and postfilters used in this approach are identical and that the corresponding reconstruction is obviously a valid form of interpolation. These observations suggest that the underlying orthogonal and cardinal representations are equivalent, which is indeed the case. In fact, we have demonstrated that the standard sampling/reconstruction paradigm for bandlimited signals corresponds to a particular form of spline interpolation for which the order tends to infinity [23]. We have also shown that among the basis functions and optimal prefilters discussed in Section III, the functions $\eta^n(x), \mathring{\eta}^n(x)$, and $\phi^n(x)$ all tend to $\mathrm{sinc}(x)$ as n goes to infinity [31]. These results also indicate that the differences between orthogonal and cardinal representations should vanish for higher order splines, which is fully consistent with our experimental observations for linear and cubic splines.

7) Relation with the Wavelet Transform: In this study, we have used the Laplacian pyramid to display the loss of information that occurs during resolution conversion. In fact, the same information can be represented in a more efficient way using the elegant method of the wavelet transform [13], [14]. This approach has the great advantage of using the same number of coefficients as does the conventional discrete signal representation. The details for the construction of an orthogonal spline wavelet transform are given in [14] and [33]. We have extended this approach for nonorthogonal polynomial spline basis functions [35]. In particular, it is possible to construct wavelets with a compact support that are the natural counterpart of the classical B-spline functions [42], [43]. Unlike Lemarié's functions, these wavelets, which are very similar to Gabor functions, do not form a fully orthogonal set. However, they still have the remarkable property of being orthogonal between resolution levels.

Finally, we note that the present construction of a multiresolution transform using nonorthogonal basis functions is not restricted to polynomial splines. It is applicable with minor modifications in the more general context of an arbitrary scaling function defined by Mallat and others.

VI. Conclusion

In this paper, we have described an extended class of polynomial spline pyramids. Each pyramid level contains the expansion coefficients of a continuous polynomial spline that provide the best (minimum L_2-norm) signal approximation at a given resolution. The decomposition in scale-space is obtained by reducing the number of parameters (spline coefficients) by a factor of two from one level to the next, which results into a fine-to-coarse sequence of signal approximations.

The algorithms that have been presented can be completely described in terms of simple linear filtering operations and sampling rate converters. For instance, the successive levels of the pyramid are generated recursively by suitable prefiltering and downsampling by a factor of two (decimation). Likewise, any coarser representation can be expanded to a higher resolution by upsampling and postfiltering (interpolation). The impulse and frequency responses of the underlying filters have been derived explicitly for polynomial splines of any order. These results should provide some general tools for the design and implementation of such systems.

A concept that has been emphasized throughout this study is that a variety of alternative (but equivalent) polynomial spline representations based on different sets of shift-invariant basis functions are available. The conversion from one representation to the other (change of coordinate system) occurs by reversible filtering. We have shown how the choice of an appropriate representation (dual or B-spline) can result in some useful simplifications of the underlying filters (e.g., simple binomial or recursive filters). Moreover, the dual spline representation provides a number of interesting links with several multiresolution techniques (scale-space filtering and Gaussian and Laplacian pyramids) that have been proposed previously.

We have shown that the selection of a modified EXPAND function, as specified by our theoretical results, can substantially reduce the energy of the Laplacian pyramid described by Burt and Adelson. These preliminary results suggest some interesting possibilities for image coding and other related image processing tasks. Polynomial spline pyramids should also be useful for the design of multigrid algorithms, which are becoming increasingly popular in a variety of applications (numerical methods, applied mathematics, and computer vision).

Appendix A
A Proof of Proposition 1

We need to show that the functions $\{\zeta^n(x-k), k \in \mathbf{Z}\}$ are linearly independent and that they form a complete set for $\mathbf{S}_1^n$.

1) Linear Independence: To prove the linear independence, we consider the equality

$$\sum_{l=-N}^{+N} c(l)\zeta^n(x-l) = 0 \qquad \forall x \in \mathbb{R}$$

which also implies that

$$\sum_{l=-N}^{+N} c(l)\zeta^n(k-l) = p * b^n * c(k) = 0 \qquad \forall k \in \mathbf{Z}.$$

It follows that $\forall k \in \mathbf{Z}, c(k) = 0$, provided that the inverse operator $(p * b^n)^{-1} = (p)^{-1} * (b^n)^{-1}$ exits, which is in accordance with our initial requirement. We note that the stability of $(b^n)^{-1}$ is guaranteed from the theoretical results in [23].

2) Completeness: This property will be demonstrated by showing that any basic basis function of $\mathbf{S}_1^n, \beta^n(x-k), k \in \mathbf{Z}$ can be expressed as a linear combination of ζ^n's. Let us consider the sum

$$\sum_{l=-\infty}^{+\infty} (p)^{-1}(l)\zeta^n(x-k-l) = \sum_{l=-\infty}^{+\infty}\sum_{l'=-\infty}^{+\infty} (p)^{-1}(l)p(l')\beta^n(x-l'-l-k).$$

By making the change of variable $k' = l' + l$, we get

$$\begin{aligned}\sum_{l=-\infty}^{+\infty} (p)^{-1}(l)\zeta^n(x-k-l) &= \sum_{l=-\infty}^{+\infty}\sum_{k'=-\infty}^{+\infty} (p)^{-1}(l)p(k'-l)\beta^n(x-k'-k)\\ &= \sum_{k'=-\infty}^{+\infty} (p)^{-1} * p(k')\beta^n(x-k'-k)\\ &= \sum_{k'=-\infty}^{+\infty} \delta_0(k')\beta^n(x-k'-k)\end{aligned}$$

which finally yields

$$\beta^n(x-k) = \sum_{l=-\infty}^{+\infty} (p)^{-1}(l)\zeta^n(x-k-l) \qquad \forall k \in \mathbf{Z}.$$

APPENDIX B
PROOF OF THEOREM 2

Since $\mathbf{S}_m^n$ is a closed subspace of $\mathbf{S}_1^n$, the process of determining the minimum L_2-norm approximation $g_m^n(x)$ of $g_1^n(x)$ is equivalent to projecting $g_1^n(x)$ into $\mathbf{S}_m^n$. Consequently, the residual error $[g_1^n(x) - g_m^n(x)]$ is orthogonal to $\mathbf{S}_m^n$, which implies that

$$\langle g_1^n(x) - g_m^n(x), \check{\zeta}_m^n(x-mk)\rangle = 0 \qquad \forall k \in \mathbf{Z}$$

or equivalently

$$\langle g_1^n(x), \check{\zeta}_m^n(x-mk)\rangle = \langle g_m^n(x), \check{\zeta}_m^n(x-mk)\rangle \qquad \forall k \in \mathbf{Z}. \tag{B1}$$

Let us first consider the left-hand side of this equality and define

$$r(l') = \langle g_1^n(x), \check{\zeta}_m^n(x-l')\rangle, \qquad l' \in \mathbf{Z}. \tag{B2}$$

By using (3.14) and (3.15), this expression is rewritten as

$$\begin{aligned} r(l') &= \left\langle \sum_{k=-\infty}^{+\infty} c_1(k) \sum_{k'=-\infty}^{+\infty} p(k')\beta^n(x-k-k'), \right.\\ &\qquad \left. \sum_{l=-\infty}^{+\infty} [\check{p}]_{\uparrow m} * u_m^n(l)\beta^n(x-l-l') \right\rangle\\ &= \sum_{k=-\infty}^{+\infty} c_1(k) \sum_{k'=-\infty}^{+\infty} p(k') \sum_{l=-\infty}^{+\infty} [\check{p}]_{\uparrow m} * u_m^n(l)\\ &\qquad \langle \beta^n(x-k-k'), \beta^n(x-l-l')\rangle.\end{aligned}$$

Using the well-known property that $\beta^n * \beta^n(x) = \beta^{2n+1}(x)$, we find that

$$\begin{aligned} r(l') = \sum_{k=-\infty}^{+\infty} c_1(k) \sum_{k'=-\infty}^{+\infty} p(k') \sum_{l=-\infty}^{+\infty} [\check{p}]_{\uparrow m}\\ * u_m^n(l)b^{2n+1}(k+k'-l-l').\end{aligned}$$

The next step is to eliminate l, k', and k by successive identification of convolution sums:

$$\begin{aligned} r(l') &= \sum_{k=-\infty}^{+\infty} c_1(k) \sum_{k'=-\infty}^{+\infty}\\ &\qquad p(k')[\check{p}]_{\uparrow m} * u_m^n * b^{2n+1}(k+k'-l')\\ &= \sum_{k=-\infty}^{+\infty} c_1(k) \sum_{k'=-\infty}^{+\infty}\\ &\qquad p(k')[\check{p}']_{\uparrow m} * u_m^n * b^{2n+1}(l'-k-k')\\ &= \sum_{k=-\infty}^{+\infty} c_1(k) * p * [\check{p}']_{\uparrow m} * u_m^n * b^{2n+1}(l'-k)\\ &= c_1 * p * [\check{p}']_{\uparrow m} * u_m^n * b^{2n+1}(l')\end{aligned} \tag{B3}$$

where $\check{p}'(k) = \check{p}(-k)$ and where the transition from the first to the second line is justified by the fact that u_m^n and b^{2n+1} are symmetrical convolution kernels. The left-hand side of (B1) is finally obtained by decimating (B3) by a factor of m

$$[r]_{\downarrow m}(k) = \check{p}' * [p * b^{2n+1} * u_m^n * c_1]_{\downarrow m}(k) \qquad \forall k \in \mathbf{Z} \tag{B4}$$

where we use the fact that $[\check{p}]_{\uparrow m\downarrow m}(k) = \check{p}(k)$.

Second, we consider the right-hand side term in (B1) and define

$$s(l') = \langle g_m^n(x), \check{\zeta}_m^n(x-l')\rangle \qquad l' \in \mathbf{Z} \tag{B5}$$

which is expanded as

$$\begin{aligned} s(l') &= \sum_{k=-\infty}^{+\infty} [\check{c}_m]_{\uparrow m}(k) \left\langle \sum_{k'=-\infty}^{+\infty} [\check{p}]_{\uparrow m} * u_m^n(k')\right.\\ &\qquad \times \beta^n(x-k-k'),\\ &\qquad \left. \sum_{l=-\infty}^{+\infty} [\check{p}]_{\uparrow m} * u_m^n(l')\beta^n(x-l-l') \right\rangle\\ &= \sum_{k=-\infty}^{+\infty} [\check{c}_m]_{\uparrow m}(k) \sum_{k'=-\infty}^{+\infty} [\check{p}]_{\uparrow m} * u_m^n(k')\\ &\qquad \times \sum_{l'=-\infty}^{+\infty} [\check{p}]_{\uparrow m} * u_m^n(l')b^{2n+1}(k+k'-l-l').\end{aligned}$$

By using the same technique as for the derivation (B3), we find that

$$s(l') = [\check{c}_m]_{\uparrow m} * [\check{p}]_{\uparrow m} * u_m^n * [\check{p}']_{\uparrow m} * u_m^n * b^{2n+1}(l'). \quad \text{(B6)}$$

We then use the convolution property of discrete B-spline kernels (2.7) to show that

$$b^{2n+1} * u_m^n * u_m^n(k) = m \cdot b_m^{2n+1}(k). \quad \text{(B7)}$$

A simplified expression for the right-hand side of (B1) is found by substituting (B7) in (B6) and performing a decimation by a factor of m:

$$\begin{aligned}[s]_{\downarrow m}(k) &= \check{p}' * \check{p} * [m \cdot b_m^{2n+1}]_{\downarrow m} \check{c}_m(k) \\ &= \check{p}' * \check{p} * m \cdot b^{2n+1} * \check{c}_m(k) \qquad \forall k \in \mathbf{Z}. \quad \text{(B8)}\end{aligned}$$

To complete our proof, we equate (B8) and (B4):

$$\begin{aligned}&m(\check{p}' * \check{p} * b^{2n+1}) * \check{c}_m(k) \\ &\qquad = \check{p}' * [p * b^{2n+1} * u_m^n * c_1]_{\downarrow m}(k) \qquad \forall k \in \mathbf{Z}\end{aligned}$$

and solve this equation by taking the inverse of the convolution operator that acts on $\check{c}_m(k)$, which finally yields (3.16). Q.E.D.

REFERENCES

[1] A. Rosenfeld, *Multiresolution Image Processing.* New York: Springer-Verlag, 1984.

[2] S. Tanimoto and T. Pavlidis, "A hierarchical data structure for picture processing," *Comput. Graphics, Image Processing,* vol. 4, pp. 104–119, 1975.

[3] C. A. Harlow and S. A. Eisenbeis, "The analysis of radiographic images," *IEEE Trans. Comput.,* vol. 22, pp. 678–688, 1973.

[4] W. Hackbush, *Multi-Grid Methods and Applications.* New York: Springer-Verlag, 1985.

[5] D. Terzopoulos, "Multilevel computational processes for visual surface reconstruction,"*Comput. Vision Graphics Image Processing,* vol. 24, pp. 52–96, 1983.

[6] R. Szeliski, "Fast surface interpolation using hierarchical basis functions," *IEEE Trans. Patt. Anal. Machine Intell.,* vol. 12, pp. 513–528, June 1990.

[7] D. Terzopoulos, "Image analysis using multigrid relaxation methods," *IEEE Trans. Patt. Anal. Mach. Intell.,* vol. PAMI-8, pp. 129–139, 1986.

[8] W. Enkelmann, "Investigations of multigrid algorithms for the estimation of optical flow fields in image sequences," *Comput. Vision Graphics Image Processing,* vol. 43, pp. 150–177, 1988.

[9] P. J. Burt and E. H. Adelson, "The Laplacian pyramid as a compact code," *IEEE Trans. Commun.,* vol. COM-31, pp. 337–345, Apr. 1983.

[10] J. L. Crowley and R. M. Stern, "Fast computation of the difference of low pass transform," *IEEE Trans. Patt. Anal. Machine Intell.,* vol. PAMI-6, pp. 212–22, 1984.

[11] M. Vetterli, "Multi-dimensional sub-band coding: some theory and algorithms," *Signal Processing,* vol. 6, pp. 97–112, Apr. 1984.

[12] J. W. Woods and S. D. O'Neil, "Sub-band coding of images," *IEEE Trans. Acoust. Speech Signal Processing,* vol. ASSP-34, pp. 1278–1288, Oct. 1986.

[13] S. G. Mallat, "Multiresolution approximation and wavelet orthogonal bases of $L^2(R)$," *Trans. Amer. Math. Soc.,* vol. 315, pp. 69–87, 1989.

[14] S. G. Mallat, "A theory of multiresolution signal decomposition: The wavelet representation," *IEEE Trans. Patt. Anal. Machine Intell.,* vol. 11, pp. 674–693, 1989.

[15] P. J. Burt, "Fast algorithms for estimating local image properties," *Comput. Graphics Image Processing,* vol. 21, pp. 368–382, 1983.

[16] M. Unser, "Description statistique de textures: application à l'inspection automatique," Ph.D. thesis, Swiss Fed. Inst. of Technol., Lausanne, Switzerland, 1984.

[17] A. P. Witkin, "Scale-space filtering," in *Proc. 4th Int. Joint Conf. Artificial Intell.,* 1983, pp. 1019–1022.

[18] J. Koenderink, "The structure of images," *Biol. Cybern.,* vol. 50, pp. 363–370, 1984.

[19] J. Babaud, A. P. Witkin, M. Baudin, and R. O. Duda, "Uniqueness of the Gaussian kernel for scale-space filtering," *IEEE Trans. Patt. Anal. Machine Intell.,* vol. PAMI-8, pp. 26–33, Jan. 1986.

[20] A. Yuille and T. Poggio, "Scaling theorems for zero-crossings," *IEEE Trans. Patt. Anal. Machine Intell.,* vol. PAMI-8, pp. 15–25, Jan. 1986.

[21] T. Lindeberg, "Scale-space for discrete signals," *IEEE Trans. Patt. Anal. Machine Intell.,* vol. 12, pp. 234–254, Mar. 1990.

[22] I. J. Schoenberg, "Cardinal interpolation and spline functions," *J. Approximation Theory,* vol. 2, pp. 167–206, 1969.

[23] A. Aldroubi, M. Unser, and M. Eden, "Cardinal spline filters: Stability and convergence to the ideal sinc interpolator," *Signal Processing,* vol. 28, pp. 127-138, Aug. 1992.

[24] I. J. Schoenberg, "Contribution to the problem of approximation of equidistant data by analytic functions," *Quart. Appl. Math.,* vol. 4, pp. 45–99; 112–141, 1946.

[25] M. Unser, A. Aldroubi, and M. Eden, "Fast B-spline transforms for continuous image representation and interpolation," *IEEE Trans. Patt. Anal. Machine Intell.,* vol. 13, pp. 277–285, Mar. 1991.

[26] I. J. Schoenberg, *Cardinal spline interpolation.* Philadelphia, PA: Soc. Indus. Applied Math., 1973.

[27] ——, "Notes on spline functions III: On the convergence of the interpolating cardinal splines as their degree tends to infinity," *Israel J. Math.,* vol. 16, pp. 87–92, 1973.

[28] P. M. Prenter, *Splines and Variational Methods.* New York: Wiley, 1975.

[29] L. L. Schumaker, *Spline Functions: Basic Theory.* New York: Wiley, 1981.

[30] B. K. P. Horn, *Robot Vision.* New York: McGraw-Hill, 1986.

[31] M. Unser, A. Aldroubi, and M. Eden, "Polynomial spline signal approximations: Filter design and asymptotic equivalence with Shannon's sampling theorem," *IEEE Trans. Inform. Theory,* vol. 38, pp. 1–9, Jan. 1992.

[32] W. K. Pratt, *Digital Image Processing.* New York: Wiley, 1978.

[33] P. -G. Lemarié, "Ondelettes à localisation exponentielles," *J. Math. Pures Appl.,* vol. 67, pp. 227–236, 1988.

[34] A. Stuart and J. K. Ord, *Kendall's Advanced Theory of Statistics–Volume 1: Distribution Theory.* New York: Oxford University Press, 1987.

[35] M. Unser, A. Aldroubi and M. Eden, "A family of polynomial spline wavelet transforms," NCRR Rep. 153/90, Nat. Inst. Health, 1990.

[36] C. de Boor, *A Practical Guide to Splines.* New York: Springer-Verlag, 1978.

[37] A. Aldroubi, M. Unser and M. Eden, "Asymptotic properties of least squares spline filters and application to multi-scale decomposition of signals," in Proc. *Int. Symp. Inform. Theory Applications* (Waikiki, HI), Nov. 27–30, 1990, pp. 271–274.

[38] M. Unser and M. Eden, "Multi-resolution feature extraction and selection for texture segmentation," *IEEE Trans. Patt. Anal. Machine Intell.,* vol. PAMI-11, pp. 717–728, July 1989.

[39] D. Marr and E. Hildreth, "Theory of edge detection," *Proc. Roy. Soc. London,* vol. B 207, pp. 187–217, 1980.

[40] A. J. Jerri, "The Shannon sampling theorem—Its various extensions and applications: A tutorial review," *Proc. IEEE,* vol. 65, pp. 1565–1596, 1977.

[41] R. E. Crochiere and L. R. Rabiner, "Interpolation and decimation of digital signals," *Proc. IEEE,* vol. 69, pp. 300–331, Mar. 1981.

[42] C. K. Chui and J. Z. Wang, "On compactly supported spline wavelets and a duality principle," *Trans. Am. Math. Soc.,* vol. 330, no. 2, pp. 903–915, 1992.

[43] M. Unser, A. Aldroubi and M. Eden, "On the asymptotic convergence of B-spline wavelets to Gabor functions," *IEEE Trans. Inform. Theory,* vol. 38, pp. 864–872, Mar. 1992.

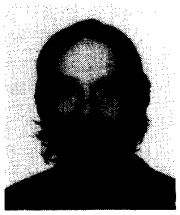

Michael Unser (M'89) was born in Zug, Switzerland, on April 9, 1958. He received the M.S. (with honors) and Ph.D. degrees in electrical engineering in 1981 and 1984, respectively, from the Swiss Federal Institute of Technology in Lausanne, Switzerland.

He is currently a Visiting Scientist with the Biomedical Engineering and Instrumentation Program, National Institutes of Health, Bethesda, MD, which he joined in 1985. He has also been affiliated with the French National Institutes of Health and Biomedical Research (INSERM) since April 1988. His research interests include the application of image processing and pattern recognition techniques to various biomedical problems, multiresolution image representations, and the use of splines in signal processing.

Dr. Unser is an Associate Editor for the IEEE TRANSACTIONS ON IMAGE PROCESSING.

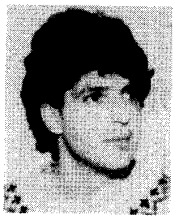

Akram Aldroubi was born in Homs, Syria, on May 20, 1958. He received the M.S. degree in electrical engineering in 1982 from the Swiss Federal Institute of Technology, Lausanne, Switzerland. He received the M.S. and Ph.D. degrees in mathematics in 1984 and 1987, respectively, from Carnegie-Mellon University, Pittsburgh, PA.

He is currently a Staff Fellow with the Biomedical Engineering and Instrumentation Program, National Institutes of Health, Bethesda, MD. His research interests include functional analysis, wavelet transforms, differential equations, signal processing, and mathematical biology.

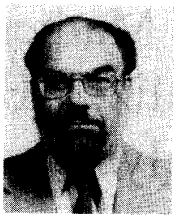

Murray Eden (M'60-F'73-LF'91) was born in Brooklyn, NY, on August 17, 1920. He received the B.S. degree from City College of New York in 1939 and the Ph.D. degree from the University of Maryland in 1951.

He is currently director of the Biomedical Engineering and Instrumentation Program, National Center for Research Resources, National Institutes of Health, and Professor of Electrical Engineering, Emeritus, Massachusetts Institute of Technology, Cambridge. His research interests include pattern recognition, analytical uses of image processing, and models for perception.